J|A|C|S
ARTICLES
Published on Web 02/14/2008

Polymerized PolyHEMA Photonic Crystals: pH and Ethanol Sensor Materials

Xiangling Xu, Alexander V. Goponenko, and Sanford A. Asher*

Department of Chemistry, University of Pittsburgh, Pittsburgh, Pennsylvania 15260

Received October 17, 2007; E-mail: asher@pitt.edu

Abstract: The surface of monodisperse silica particles synthesized using the Stober process were coated with a thin layer of polystyrene. Surface charge groups were attached by a grafting polymerization of styrene sulfonate. The resulting highly charged monodisperse silica particles self-assemble into crystalline colloidal arrays (CCA) in deionized water. We polymerized hydroxyethyl methacrylate (HEMA) around the CCA to form a HEMA-polymerized crystalline colloidal array (PCCA). Hydrofluoric acid was utilized to etch out the silica particles to produce a three-dimensional periodic array of voids in the HEMA PCCA. The diffraction from the embedded CCA sensitively monitors the concentration of ethanol in water because the HEMA PCCA shows a large volume dependence on ethanol due to a decreased Flory−Huggins mixing parameter. Between pure water and 40% ethanol the diffraction shifts across the entire visible spectral region. We accurately modeled the dependence of the diffraction wavelength on ethanol concentration using Flory theory. We also fabricated a PCCA (which responds to pH changes in both low and high ionic strength solutions) by utilizing a second polymerization to incorporate carboxyl groups into the HEMA PCCA. We were also able to model the pH dependence of diffraction of the HEMA PCCA by using Flory theory. An unusual feature of the pH response is a hysteresis in response to titration to higher and lower pH. This hysteresis results from the formation of a Donnan potential at high pH which shifts the ionic equilibrium. The kinetics of equilibration is very slow due to the ultralow diffusion constant of protons in the carboxylated PCCA as predicted earlier by the Tanaka group.

We are developing chemical sensors by creating photonic crystals within chemically responsive hydrogels.[1−14] We fabricate these photonic crystal sensors through the self-assembly of a crystalline colloidal array (CCA) of monodisperse particles which form an fcc lattice which Bragg diffracts light. We generally create an fcc lattice whose 111 plane diffracts in the visible spectral region. We then polymerize a hydrogel around the CCA to form a polymerized crystalline colloidal array (PCCA). This responsive PCCA photonic crystal material possesses the volume phase-transition phenomenology of polymer hydrogels.[15−22] We attach molecular recognition agents to the hydrogel that actuate volume changes in the hydrogel which causes changes in the CCA lattice constant which can be sensitively monitored by the shifts in the wavelength of the Bragg diffracted light. We previously fabricated PCCA sensitive to temperature,[9] light,[11,12,25−27] magnetic fields,[28,29] different chemical analytes,[3,6,7,30] including important clinical analytes such as creatinine,[8] glucose,[4−7] and nerve gas agents.[31]

For example, we earlier fabricated a pH sensor by hydrolyzing a polyacrylamide hydrogel PCCA to introduce carboxyl groups.[10]

(1) Asher, S. A.; Holtz, J. H.; Liu, L.; Wu, Z. J. *J. Am. Chem. Soc.* **1994**, *116*, 4997−4998.
(2) Holtz, J.; Weissman, J.; Pan, G.; Asher. S. A. *Mater. Res. Soc.* **1998**, *23*, 44−50.
(3) Asher, S. A.; Shrama, A. C.; Goponenko, A. V.; Ward, M. M. *Anal. Chem.* **2003**, *75*, 1676−1683.
(4) Asher, S. A.; Alexeev, V. L.; Goponenko, A. V.; Sharma, A. C.; Lednev, I. K.; Wilcox, C. S.; Finegold, D. V. *J. Am. Chem. Soc.* **2003**, *125*, 3322−3329.
(5) Alexeev, V. L.; Sharma, A. C.; Goponenko, A. V.; Das, S.; Lednev, I. K.; Wilcox, C. S.; Finegold, D. V.; Asher, S. A. *Anal. Chem.* **2003**, *75*, 2316−2323.
(6) Holtz, J. H.; Asher, S. A. *Nature* **1997**, *389*, 829−832.
(7) Holtz, J. H.; Holtz, J. S. W.; Munro, C. H.; Asher, S. A. *Anal. Chem.* **1998**, *70*, 780−791.
(8) Sharma, A. C.; Jana, T.; Kesavamoorthy, R.; Shi, L. J.; Virji, M. A.; Finegold, D. V.; Asher, S. A. *J. Am. Chem. Soc.* **2004**, *126*, 2971−2977.
(9) Weissman, J. M.; Sunkara, H. B.; Tse, A. S.; Asher, S. A. *Science* **1996**, *274*, 959−960.
(10) Lee, K.; Asher, S. A. *J. Am. Chem. Soc.* **2000**, *122*, 9534−9537.
(11) Pan, G.; Kesavamoorthy, R.; Asher, S. A. *Phys. Rev. Lett.* **1997**, *78*, 3860−3863.
(12) Pan, G.; Kesavamoorthy, R.; Asher, S. A. *J. Am. Chem. Soc.* **1998**, *120*, 6525−6530.
(13) Liu, L.; Li, P.; Asher, S. A. *Nature* **1998**, *397*, 141−144.
(14) Liu, L.; Li, P.; Asher, S. A. *J. Am. Chem. Soc.* **1999**, *121*, 4040−4046.
(15) Annaka, M.; Tanaka, T. *Nature* **1992**, *355*, 430−432.
(16) English, A. E.; Tanaka, T.; Edelman, E. R. *J. Chem. Phys.* **1997**, *107*, 1645−1654.
(17) Kudaibergenov, S. E.; Sigitov, V. B. *Langmuir* **1999**, *15*, 4230−4235.
(18) Mafe, S.; Manzanares, J. A.; English, A. E.; Tanaka, T. *Phys. Rev. Lett.* **1997**, *79*, 3086−3089.
(19) Lee, Y. J.; Braun, P. V. *Adv. Mater.* **2003**, *15*, 563−566.
(20) Lee, Y. J.; Pruzinsky, S. A.; Braun, P. V. *Langmuir* **2004**, *20*, 3096−3106.
(21) Takeoka, Y.; Watanabe, M. *Adv. Mater.* **2003**, *15*, 199−201.
(22) Saito, H. T. Y.; Watanabe, M. *Chem. Commun.* **2003**, 2126−2127.
(23) Flory, P. J.; Flory, P. J. *Principles of Polymer Chemistry*; Cornell University Press: Ithaca, NY, 1953; pp 432−594.
(24) Flory, P. J. *J. Chem. Phys.* **1977**, *66*, 5720−5729.
(25) Kamenjicki, M.; Asher, S. A. *Macromolecules* **2004**, *37*, 8293−8296.
(26) Kamenjicki, M.; Lednev, I. K.; Asher, S. A. *J. Phys. Chem. B* **2004**, *108*, 12637−12639.
(27) Reese, C.; Mikhonin, A.; Kamenjicki, M.; Tikhonov, A.; Asher, S. A. *J. Am. Chem. Soc.* **2004**, *126*, 1493−1496.
(28) Xu, X. L.; Friedman, G.; Humfeld, K.; Majetich, S. A.; Asher, S. A. *Adv. Mater* **2001**, *13*, 1681−1684.
(29) Xu, X. L.; Majetich, S. A.; Asher, S. A. *J. Am. Chem. Soc*. **2002**, *124*, 13864−13868.
(30) Reese, C. E.; Baltusavich, M. E.; Keim, J. P.; Asher, S. A. *Anal. Chem.* **2001**, *73*, 5038−5042.
(31) Walker, J. P.; Asher, S. A. *Anal. Chem.* **2005**, *77*, 1596−1600.

10.1021/ja077979+ CCC: $40.75 © xxxx American Chemical Society

As the pH increases, these carboxyl groups ionize to carboxylate anions that results in a Donnan potential which creates an osmotic pressure to swell the hydrogel and shift the Bragg diffraction. Unfortunately, this pH sensor only functions in low ionic strength solutions because the Donnan potential becomes negligible at high ionic strengths.

We fabricated a PCCA pH sensor that works in high ionic strength medium by attaching nitrophenol groups onto the PCCA polyacrylamide backbone.[8] At higher pH, the phenol groups dissociate to increase the hydrogel free energy of mixing, since the solubility in water of phenolates exceeds that of phenol. In 150 mM NaCl solution, the Bragg diffraction of PCCA shifts from ~470 nm to ~590 nm for pH increases from 4.4 to 9.1.

In the work here, we report the development of a new ethanol sensor as well as a new PCCA pH sensor that can be utilized in high ionic strength solution. For the first time we utilized the more biocompatible polyHEMA hydrogel which is highly responsive to ethanol. Via a second polymerization process, we incorporated carboxyl groups within the HMEA hydrogel for use in pH sensing.

Experimental Section

Synthesis of Monodisperse and Surface-Charged Silica Particles. Monodisperse SiO_2 particles were prepared by hydrolysis of tetraethyl orthosilicate (TEOS, Aldrich) in an ethanol medium in the presence of water and ammonia.[32,33] For example, a mixture of 1 L of H_2O and 45 mL of 17 M NH_3H_2O was poured into a mixture of 300 mL of TEOS and 2.7 L of ethanol at room temperature under magnetic stirring. The resulting monodisperse SiO_2 spheres were then surface coated with 3-(trimethoxysilyl)propyl methacrylate (MPS, Aldrich) to attach polymerizable vinyl groups onto the silica surfaces.

The resulting silica particles were then coated with a thin polystyrene shell through dispersion polymerization of styrene (St, Aldrich).[34] In one example, the surface-functionalized silica particles, dispersed in ethanol (250 mL, containing 4.0 g of silica particles) were mixed with 0.6 g of polyvinylpyrrolidone (PVP, MW 360 K, Aldrich), 0.2 g of 2,2′-azo-bis-isobutyronitrile (AIBN, Aldrich), 0.1 g of St, and then heated to 60 °C for 24 h under stirring.

The silica/polystyrene core/shell composite particle surfaces were functionalized with sulfonic acid groups via graft polymerization of sodium styrene sulfonate (SSS, Polysciences). A 5-mL ethanol dispersion containing 2 g of colloid particles was mixed with 45 mL of an aqueous solution containing 0.3 g of ammonium persulfate (APS, Aldrich) and 0.5 g of SSS. The resulting mixture was incubated in a 65 °C water bath for 3 h. The particles were then extensively washed by repeated centrifugation and ultrasonic dispersion in water.

Preparation of HEMA-PCCA. The PCCAs were synthesized by UV polymerization of hydroxyethylmethacrylate (HEMA, Polysciences Inc.) utilizing diethoxyacetophenone (DEAP) as a photoinitiator.[1] A typical recipe utilized 0.34 g of HEMA, 0.017 g of poly(ethylene glycol)$_{200}$ dimethacrylate (PEGDMA, Polysciences Inc.), and 1 g of the silica CCA suspension (13 vol %) in deionized water. This dispersion was injected into a cell consisting of two clean quartz disks separated by a 125-μm Parafilm spacer. Photopolymerization was performed using UV mercury lamps [Black Ray (365 nm)] for 40−60 min.

The resulting HEMA-PCCA was further modified by a second polymerization to incorporate carboxyl groups into the hydrogel matrix. The HEMA-PCCA film was immersed in the mixture of HEMA, PEGDMA, acrylic acid, and DEAP in water for 12 h. The film was then polymerized by exposure to UV light for 30 min. This second polymerization forms an interpenetrating network inside the HEMA-PCCA film. In order to increase the diffracted light intensity, after the second polymerization, we removed the silica particles inside the PCCA by etching with HF.

Measurements. Particle diameters were determined by transmission electron microscopy (Zeiss EM902 electron microscope). The surface charge density of the silica particles was determined by conductometric titrations of purified colloid samples with 0.01 N sodium hydroxide solution. A Brookhaven Z-90 plus light-scattering photometer was used to measure the ζ-potentials. Reflectance diffraction spectra were measured using a 6 around 1 reflectance probe by using a 440 CCD spectrophotometer (Spectral Instruments, Inc.). Transmission measurements were measured with Cary 5000 UV−vis−NIR spectrophotometer (Varian Inc.). During measurements, the CCA and PCCA samples were oriented normal to the incident light beam.

Results and Discussion

CCA and PCCA Based on Surface-Charged Silica Colloid Particles. Submicrometer monodisperse silica colloidal particles can be synthesized through either the Stober process in ethanol media[32,33] or in microemulsion systems.[35,36] Most previous photonic crystal studies utilizing monodisperse silica particles use very high-volume fractions where the silica colloids self-assemble into three-dimensional (3D) close-packed arrays. There are only a few studies on the self-assembly of electrostatically stabilized silica CCA,[35,37−39] due to the previous lack of reliable, simple processes to functionalize the silica particle surfaces with strong acid groups.

In the work here, we report a reliable procedure to functionalize monodisperse silica surfaces with sulfonic acid groups. Silica particles are first coated with a ~2-nm thin polystyrene layer (determined by the ratio of Sty monomer/silica colloid volume),[34] which is further surface modified by a grafting polymerization of styrene sulfonate. TEM measurements show that the ~138-nm diameter silica particles have a 6% polydispersity. The measured ζ potential of these silica particles in 1 mM KCl was −53 mV. The charge density measured with conductometric titration was 0.9 μC/cm^2, which corresponds to 3400 sulfonates/particle.

The resulting monodisperse silica particles self-assemble into a CCA in deionized water, due to the long-range electrostatic repulsions between particles. Figure 1 shows the dependence of the diffraction wavelength on the volume fraction of silica particles measured by transmission spectra. The diffraction efficiency of the silica CCA is much lower than CCA of monodisperse, highly surface-charged polystyrene particles because of the smaller refractive index difference between the silica particles ($n = 1.387$, see below) and water ($n = 1.333$).

As the volume fraction decreases, the diffraction wavelength red-shifts from 563 to 1374 nm, while the diffraction efficiency decreases dramatically, as expected due to the decrease in the particle diameter relative to the diffracted wavelength.

The 3D periodic silica CCA was embedded in a hydrogel (Figure 2) by photopolymerizing HEMA and PEGDMA around the silica particles.[1] Before polymerization, the CCA diffraction peak appears at 592 nm in the transmission spectrum. After 30

(32) Stober, W. F.; Bohn, E. J. *J. Colloid Interface Sci.* **1968**, *26*, 62.
(33) van Blaaderen, A.; Kentgens, A. P. M. *J. Non-Cryst. Solids* **1992**, *149*, 161−178.
(34) Xu, X. L.; Asher, S. A. *J. Am. Chem. Soc.* **2004**, *126*, 7940−7945.
(35) Wang, W.; Asher, S. A. *J. Am. Chem. Soc.* **2001**, *123*, 12528−12535.
(36) Chang, S. Y.; Liu, L.; Asher, S. A. *J. Am. Chem. Soc.* **1994**, *116*, 6739−6744.
(37) Wang, W.; Cu, B.; Liang, L.; Hamilton, W. *J. Phys. Chem. B* **2003**, *107*, 3400−3404.
(38) Beck, C.; Hartl, W.; Hempelamnn, R. *Angew. Chem., Int. Ed.* **1999**, *38*, 1297−1300.
(39) Kim., S. B.; Kim, D. P. *J. Sol.-Gel Sci. Technol.* **2003**, *26*, 89−93.

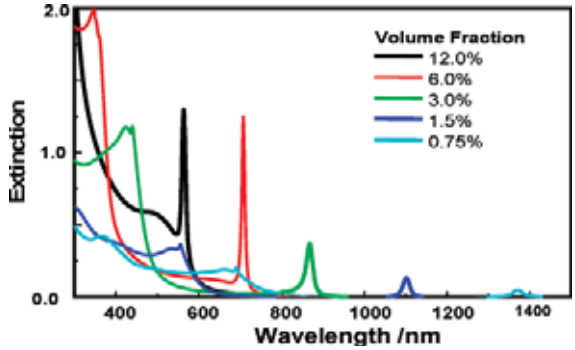

Figure 1. 1. Transmission spectra of CCA of 138 nm silica spheres with 3.4×10^3 surface sulfonates/particle at different volume fractions. These extinction peaks, which are diffracted by the fcc 111 planes, red-shift upon dilution, while the diffraction intensity decreases.

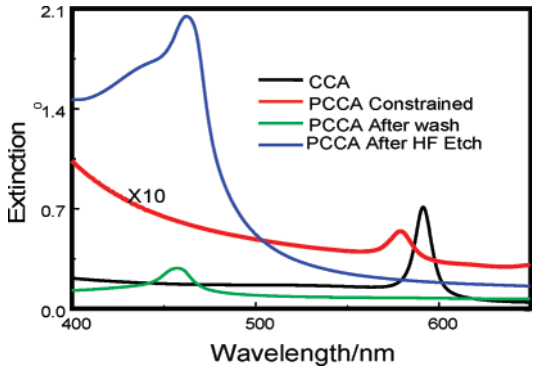

Figure 2. Transmission spectra of CCA of silica particles before and after polymerization indicate that the CCA ordering is well preserved after polymerization. After removing the silica with HF, the diffraction intensity greatly increases due to the increased refractive index mismatch between the hydrogel and the water holes.

min photopolymerization, a clear PCCA film was produced. The refractive index of pure polyHEMA is 1.512,[40] while the refractive index of the hydrogel can be calculated as $n \approx \sum \phi_i n_i \approx 1.382$, where ϕ_i and n_i are the volume fraction and the refractive indices, respectively, of each component. The calculated refractive index of the system is very close to that of the silica colloidal particles (1.387, see below). Therefore, only a very weak 580-nm diffraction peak is observed.

When the polymerization cell was opened and the hydrogel was freed and washed with water, the hydrogel film shrinks and the diffraction peak further blue-shifts to 458 nm. The increased polyHEMA concentration in the shrunken PCCA increases the refractive index, which increases the refractive index mismatch between the silica particles (1.387) and the hydrogel−water medium (1.398). Therefore the diffraction peak extinction increases.

Figure 2 shows that removing the silica colloidal particles with HF leaves water holes which more efficiently diffract at 462 nm because the refractive index mismatch between the water holes (water, 1.333) and the hydrogel medium (1.398) increases dramatically.

Ethanol-Sensing PCCA. Figure 3 shows that the diffraction of a HEMA-PCCA containing a CCA of spherical water holes or of silica particles red-shifts as the ethanol content increases from pure water to 40% ethanol. This swelling results from the increased favorable free energy of mixing of the HEMA with ethanol than with water. We can easily detect the presence of 1% ethanol.

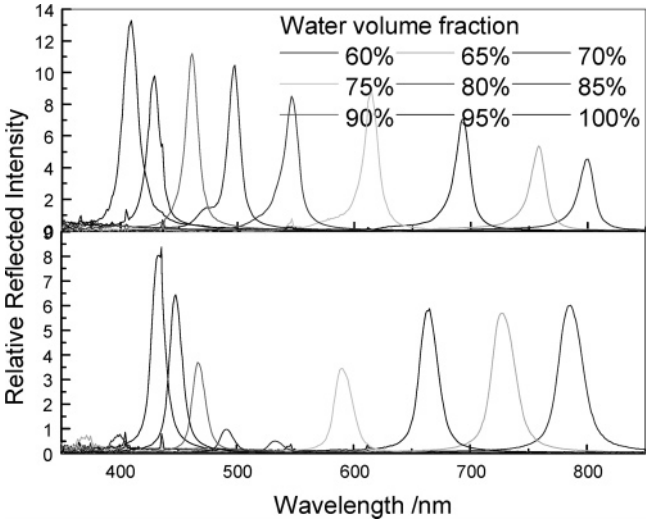

Figure 3. Dependence of diffraction of polyHEMA PCCA containing solvent voids (top), or silica particles (bottom) on the aqueous solution ethanol concentration. Note that the diffraction almost completely disappears for the silica PCCA upon refractive index matching which occurs at an ~20% ethanol volume fraction.

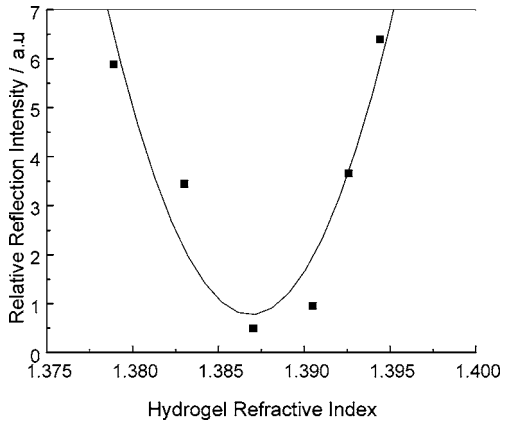

Figure 4. Dependence of relative diffraction intensity of the silica particle PCCA on the calculated refractive index of the polyHEMA hydrogel medium. The diffraction is a minimum when the refractive index of hydrogel medium matches that of the silica particles (1.387).

In the case of the PCCA with the spherical water voids, the diffraction efficiency monotonically decreases as the hydrogel swells since the refractive index difference between the HEMA hydrogel and the solvent holes monotonically decreases as the ethanol concentrations increases (n_{water} =1.33, n_{EtOH} = 1.36, n_{HEMA} = 1.51).

In contrast, the diffraction intensity of the PCCA with the silica CCA shows a vanishingly small diffraction intensity for an ethanol volume fraction of ~20 vol %. At this concentration of ethanol the HEMA hydrogel/solvent system has the same refractive index as the silica particles. At higher ethanol concentrations further swelling occurs, and the overall refractive index of HEMA-hydrogel/solvent matrix decreases below that of silica which further increases the refractive index mismatch between the silica and the hydrogel solution medium. We modeled (Figure 4) the dependence of the diffraction intensity on the refractive index of the hydrogel matrix n_m as varying

(40) Brandrup, J.; Immergut, E. H.; Grulke, E. A. *Polymer Handbook*, 4th ed; John Wiley & Sons Inc: New York, 1998.

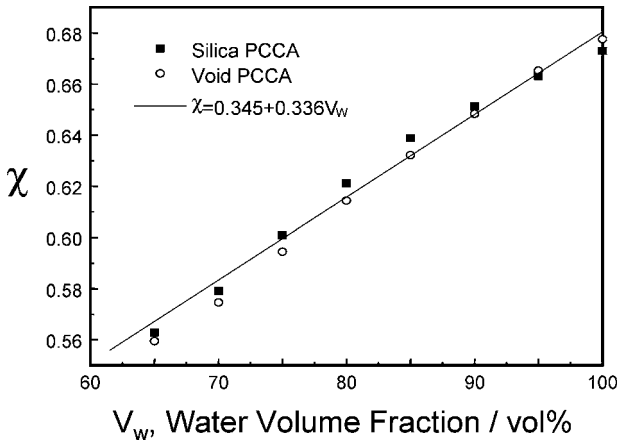

Figure 5. Flory−Huggins parameter χ for HEMA PCCA of silica spheres and for a HEMA PCCA of water voids in ethanol water solutions of water volume fraction, V_w calculated from data shown in Figure 3.

with the square of the refractive index mismatch and found a best fit:[14,41,42] $I = 8.94 \times 10^4(n_m - 1.387)^2 + 0.77$.

This result indicates that the refractive index of our silica colloid particles is 1.387, which is significantly smaller than the typical refractive index (∼1.44 for 106-nm Stober silica) reported by van Helden.[41] This difference may result from our different synthesis conditions. In our case the water concentration (∼14 M) greatly exceeds the ammonia concentration (∼0.2 M), while they are similar in van Helden's system (water, ∼3 M; ammonia, ∼3 M). In addition, the porosity of Stober silica spheres is known to increase with size.[41]

We can model the diffraction wavelength dependence of these two PCCAs on the ethanol/water concentrations.[4,5,8,10] The equilibrium volume of the nonionic HEMA PCCA is determined by the condition that the total hydrogel osmotic pressure, $\Pi_T = \Pi_M + \Pi_E = 0$, where Π_M is the osmotic pressures due to the free energy of mixing and Π_E is the hydrogel network elastic restoring force. Since one side of PCCA is attached to the quartz plate, the hydrogel can only deform in one dimension, whereas the other dimensions remain constant.[43]

$$\Pi_M = -\frac{\partial \Delta G_M}{\partial V} = -\frac{RT}{V_s}\left[\ln\left(1-\frac{V_0}{V}\right)+\frac{V_0}{V}+\chi\left(\frac{V_0}{V}\right)^2\right] \quad (1)$$

$$\Pi_E = -\frac{\partial \Delta G_E}{\partial V} = -\frac{RT\cdot n_{cr}}{V_m}\left[\left(\frac{V}{V_m}\right)-\frac{1}{2}\frac{V_m}{V}\right] \quad (2)$$

where R is universal gas constant, T is the temperature, χ is the Flory−Huggins interaction parameter for the polymer network and the solution, V_s is the molar volume of the solvent, n_{cr} is the effective number of cross-linked chains in the network, V is the existing volume of the hydrogel (not including the embedded silica colloidal particles or the voids), V_m is the volume of the relaxed hydrogel matrix, and V_0 is the volume of the dry polymer network.

We make the crucial assumptions that the hydrogel polymerization occurs under conditions where the cross-linked chain length distribution is in its statistically most probable configuration such that the volume of the prepared gel (before washing) is equal to V_m. In our case, after polymerization, the

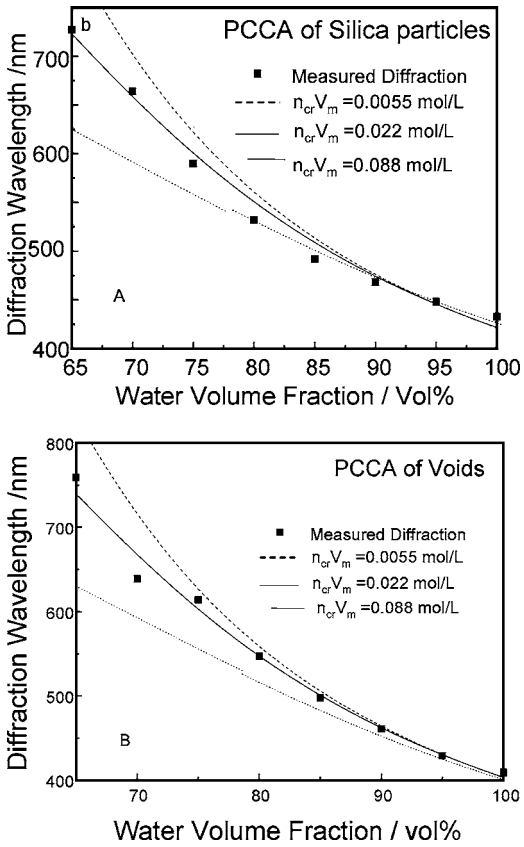

Figure 6. Modeled response of HEMA PCCA to water volume fraction for different cross-link densities. (A) Silica particle PCCA. (B) Spherical void PCCA. $\chi = 0.345 + 0.336\ V_W$.

PCCA has a diffraction of $\lambda_{ref} = 580$ nm, which corresponds to a PCCA where the silica particles occupy 9.9% of the volume, the HEMA polymer occupies 23.6% of the volume, while the rest is water. We initially calculate $n_{cr}/V_m = 0.022$ mol/L from the crosslinker to HEMA stoichiometry, but consider the possibility that n_{cr}/V_m could dramatically differ from this value.

We can calculate the total volume, V_T of the PCCA from the diffracted wavelength λ. From this we can calculate the hydrogel volume of the PCCA with silica particles is $V = V_T - V_{col} = V_m\,(\lambda n_{ref})/(\lambda_{ref} n) - V_{col}$, whereas for the PCCA with voids $V = V_T - V_{col} \cong V_m(\lambda n_{ref})/(\lambda_{ref} n) - V_{col}$, where n_{ref} is the refractive index of the PCCA with the original diffraction of $\lambda_{ref} = 580$ nm and n is the refractive index of the PCCA diffracting at λ and V_{col} is the volume of the PCCA taken up by the colloidal particles (or voids).

We can use eqs 1 and 2 to calculate the Flory−Huggins parameter, χ, for the HEMA PCCA for different ethanol/water mixtures (Figure 5). The χ values calculated for our PCCA of silica particles are very close to those calculated for the PCCA of spherical voids. χ increases linearly with the water volume fraction, V_W, $\chi = 0.345 + 0.336V_W$. The calculated value of χ for polyHEMA in pure water of 0.681 is significantly below the reported value of 0.8.[44,45] This may result from our incorporation of the longer, more hydrophilic cross-linker

(41) Van de Hulst, H. C. *Light Scattering by Small Particles*; Dover Publications: New York, 1981.
(42) Pan, G.; Tse, A. S.; Kesavamoorthy, R.; Asher, S. A. *J. Am. Chem. Soc.* **1998**, *120*, 6518−6524.
(43) Goponenko, A. V.; Asher, S. A. *J. Am. Chem. Soc.* **2005**, *127*, 10753−10759.
(44) Tauer, K.; Ali, A. M. I.; Sedlak, M. *Colloid Polym. Sci.* **2005**, *283*, 351−358.
(45) Lee, J. W.; Kim, E. H.; Jhon, M. S. *Bull. Korean Chem. Soc.* **1983**, *4*, 162−169.

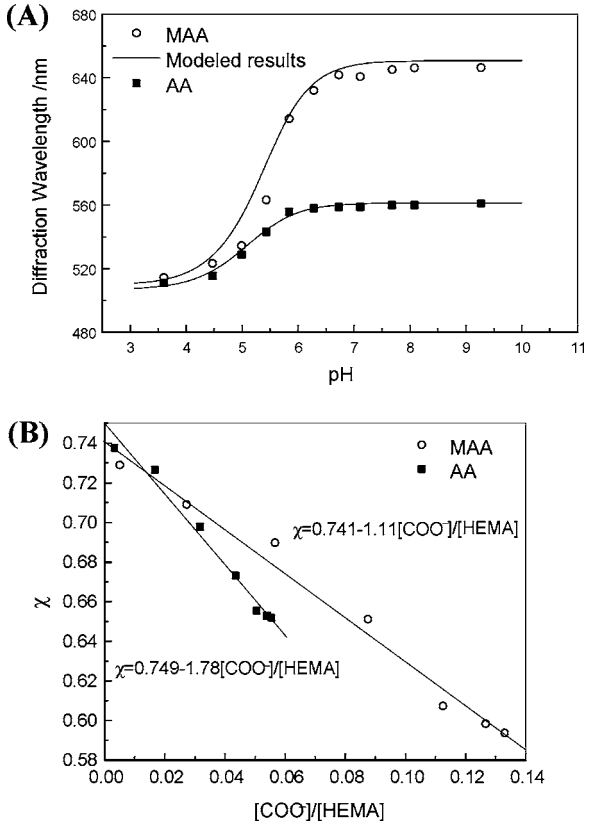

Figure 7. (A) pH dependence of HEMA PCCA hydrogel containing 5.6 mol % AA or 13.1 mol % MAA in 150 mM NaCl with 100 mM PBS buffer. (B) Variation of Flory−Huggins parameter vs the carboxylate group concentration inside the hydrogel for high ionic strength solutions.

PEGDMA, compared to the more hydrophobic crosslinkers used previously.[44,45]

Figure 6 shows the experimentally determined dependence of the diffraction wavelength of these two PCCA on the volume fraction of water calculated by using eqs 1 and 2 with the χ values found in Figure 5 for a range of cross-link densities, n_{cr}/V_m 4-fold smaller and larger than the stoichiometrically calculated value. The modeling is significantly better at the stoichiometric cross-link densities.

HEMA PCCA pH Sensor. We fabricated a PCCA pH sensor which operates even in high ionic strength solutions by incorporating carboxyl groups into the PCCA via a second polymerization which creates an interpenetrating network. This pH response results because the free energy of mixing the hydrogel becomes more favorable as the carboxyl groups titrate at higher pH values. The change in χ is more pronounced for MMA because χ changes much more dramatically than for AA going from very hydrophobic to hydrophilic as the carboxyl groups titrate.

The pH-sensing PCCA was fabricated by incubating the HEMA silica PCCA in an aqueous solution of HEMA (5 wt %), AA or MMA (1 wt %), and PEGDMA (0.25 wt %) containing a UV initiator for 12 h. After 12 h the PCCA was exposed to UV light for 30 min. The silica particles in the resulting PCCA were removed by immersing the PCCA in 1% HF aqueous solution for 5 min to increase the diffraction intensity.

Figure 7A shows the pH dependence of diffraction from this PCCA in a 100 mM phosphate buffer solution containing 150 mM NaCl. We fabricated two PCCAs, one in which we incorporated poly(acrylic acid) (AA) while in the other we incorporated polymethacrylic acid (MAA). As the pH increases, the Bragg diffraction wavelength red-shifts.

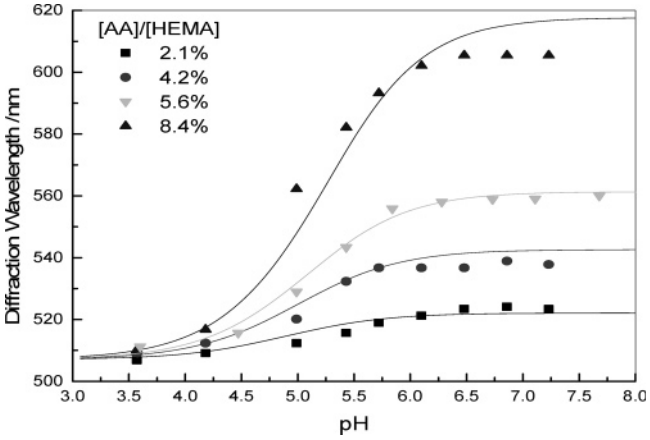

Figure 8. Modeled (solid lines) and experimentally observed pH response of HEMA PCCA hydrogel containing different loadings of AA in 150 mM NaCl with 100 mM PBS buffer.

The Donnan potential resulting from the ionization of carboxyl groups is not significant at these high ionic strength solutions. The swelling observed results from the increased solubility of carboxylates compared to carboxyl acid groups which decrease the Flory−Huggins χ free energy of mixing parameter.

Since these PCCA are free in solution and can change volume in all three dimensions. we must replace the 1D swelling elastic restoring force Π_E in eq 2 by the expression for 3D swelling[23]

$$\Pi_E = -\frac{\partial \Delta G_E}{\partial V} = -\frac{RT \cdot n_{cr}}{V_m}\left[\left(\frac{V_m}{V}\right)^{1/3} - \frac{1}{2}\frac{V_m}{V}\right] \qquad (3)$$

We modeled the swelling behavior by calculating the Flory−Huggins parameter χ at each pH by using eqs 1 and 3. By assuming identical pH values inside and outside of PCCA, and by assuming a dissociation constant K_a of 1.6×10^{-5}, identical to that of propionic acid, we calculated the concentration of carboxylate inside the gel. Figure 7B shows the calculated χ value vs the calculated molar ratio of carboxylate to HEMA groups within the hydrogel. The Flory−Huggins parameter χ decreases linearly as the concentration of carboxylates increases with addition of AA and MAA. Using the calculated χ parameter we modeled the overall pH dependence as shown in Figure 7A.

We also fabricated PCCA pH sensors with different loadings of AA. Given the observed dependence of χ on the carboxylate concentration, $\chi = 0.749 - 1.78[COO^-]/[HEMA]$, we modeled the pH dependence of these PCCA in 150 mM NaCl containing 100 mM phosphate buffer. As shown in Figure 8, the modeled values are very close to the measured data.

We also measured the pH response of the PCCA in low ionic strength media. As expected, the response at low ionic strength is much larger than that at high ionic strength, because the Donnan potential associated with the dissociation of the carboxyl acid group in the hydrogel selectively contributes at low ionic strengths. The total osmotic pressure for a charged hydrogel is given by: $\Pi_T = \Pi_M + \Pi_E + \Pi_{Ion} = 0$.

For a dilute solution, Π_{Ion} can be approximated by[23]

$$\Pi_{Ion} = RT(c_+ + c_- - c^*_+ - c^*_-) \quad (4)$$

where c_+ and c_- are the concentrations of the mobile cation and mobile anion inside the gel, and c^*_+ and c^*_- are their concentrations outside the gel. In the case here, we use the simplifying conditions that all ionic species are singly charged and the anion/cation stoichiometry is unity. From electrostatic neutrality, the relation between the concentration of mobile cations and anions in the gel is

$$c_+ = c_- + c_{de}, \quad c^*_+ = c^*_-, \quad c_{de} = \frac{K_a C_T}{K_a + [H^+]} \quad (5)$$

where c_{de} is the concentration of dissociated carboxyl group in the hydrogel, K_a is the dissociation constant of the carboxyl groups, C_T is the total concentration of carboxyl groups inside the gel, which is inversely proportional to the hydrogel volume, $C_T = n_T/V$, and $[H^+]$ is the hydrogen ion concentration inside the hydrogel.

Rather than obtaining the Donnan ratio, c^*_A/c_A from the Donnan potential,[46] we more conveniently determine it by invoking equality of electrolyte activity inside and outside the hydrogel, $c_+c_- = c^*_+c^*_-$. The electrolyte activity, here approximated as the ion concentrations, is the product of the activities of the individual dissociated ions. We obtain

$$c_+ = \frac{c^*_-}{c_-} c^*_+ [H^+] = \frac{c^*_-}{c_-} [H^+]^*$$

where [H+] and [H+]* are the hydrogen ion concentrations inside and outside the hydrogel, respectively.

For an infinite reservoir volume with defined composition we can directly calculate the concentration of ions inside the PCCA and calculate Π_{Ion} at any hydrogel volume. If the reservoir volume is finite, we can calculate the concentrations by considering the mass balance.

We calculated the dependence of the Flory−Huggins parameter χ vs the carboxylate group concentration in low ionic strength media from the results in Figure 9A. We assumed that the PCCA is dispersed in an infinite reservoir. For each pH, we can calculate the volume of the PCCA (V) from the diffracted wavelength, λ:

$$V = \frac{(\lambda n_{ref})}{(\lambda_{ref} n)(V_m - V_{col})}$$

By initially assuming the $[H^+]$ is identical to $[H^+]^*$, we can calculate the extent of carboxylate ionization c_{de}:

$$c_{de} = \frac{(K_a C_T)}{(K_a + [H^+])}$$

Since

$$c_+ = c_- + c_{de}, \quad c^*_+ = c^*_-, \quad c_+ = (c^*_-)/(c_-)c^*_+$$

we can calculate c_-. With $[H^+] = (c^*_-)/(c_-)[H^+]^*$, we can iterate the $[H^+]$. Though iteration, we found $[H^+]$ and all the other parameters needed to calculate Π_{Ion}. We calculated χ in Figure 9B by utilizing the equilibrium relationship $\Pi_T = \Pi_M + \Pi_E + \Pi_{Ion} = 0$.

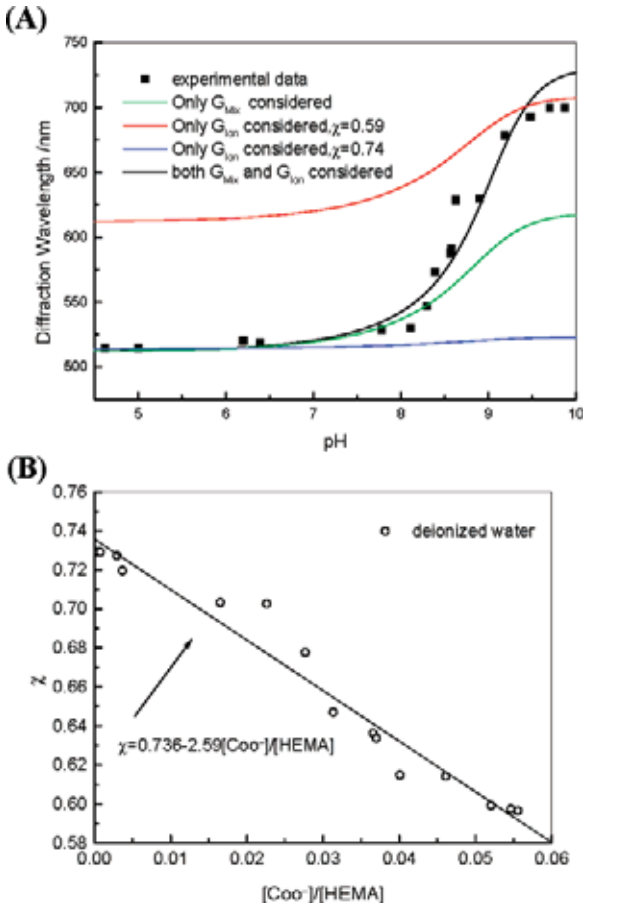

Figure 9. (A) Modeled (solid black line) and experimentally observed pH dependence of diffraction from a HEMA PCCA hydrogel containing 5.63 mol % AA in a solution containing deionized water and the acid required to establish pH 4.5 followed by the base required to increase the pH to the valued desired. Green shows modeling which only includes contributions from the free energy of mixing (G_{Mix}). Red line considered only ionic contributions with χ fixed at 0.59. The green line considered only ionic contributions with χ fixed at 0.74. (B) Dependence of Flory−Huggins χ parameter vs the carboxylate concentration inside the hydrogel for low ionic strength media.

As shown in Figure 9B, χ decreased linearly as the carboxylate group concentration increased within the gel. Given the pH dependence of χ in Figure 9B, we can easily model the response of the PCCA in low ionic strength solution (Figure 9A). In Figure 9A, we also show the response which would occur in the case where only G_{Mix} or G_{Ion} (χ fixed at 0.59 or 0.74) contributes to the hydrogel volume change. It is clear that the contribution from variations in G_{Mix} variation is more important than that from variations in G_{Ion}.

pH Response Hysteresis. The pH response of PCCA showed hysteresis in low ionic strength solutions as shown in Figure 10. For this measurement we titrated the PCCA in pure water with NaOH until it reached pH = 10 in order to ensure conversion of all carboxyl groups inside the PCCA to carboxylates ($V_{bath}/V_{gel} = 10^4$). We then titrated the PCCA to lower pH by adding aliquots of HCl, followed by measuring the diffraction after 1 h increments. We compared the resulting titration behavior to that of a PCCA which was first poised at pH = 3.5

(46) Ricka, J.; Tanaka, T. *Macromolecules* **1984**, *17*, 2916−2921.

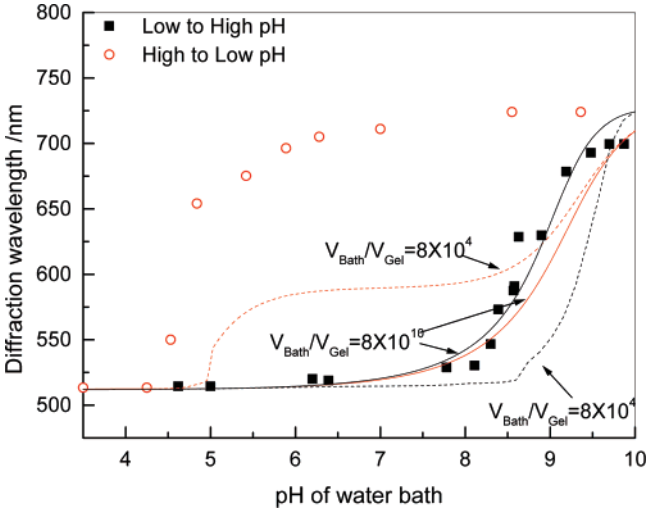

Figure 10. Modeled and experimental pH dependence of diffraction wavelength of HEMA PCCA hydrogels containing 5.63 mol % AA in low ionic strength media. Experimental (red scattered circle) and modeling (red dashed line) response of PCCA with all carboxyl groups in carboxylate form, when dispersed in pH 10 reservoir ($V_{bath}/V_{gel} = 8 \times 10^4$) and then pH was decreased with HCl, while the red solid line shows the modeling response if the reservoir is infinite ($V_{bath}/V_{gel} = 8 \times 10^{10}$). Black dashed line shows the modeling Bragg diffraction if the same PCCA gel dispersed in a pH 4 reservoir ($V_{bath}/V_{gel} = 8 \times 10^4$) and then pH was increased with NaOH. Experimental (black scattered squares) and modeling (black solid line) response of the same PCCA if the reservoir is infinite.

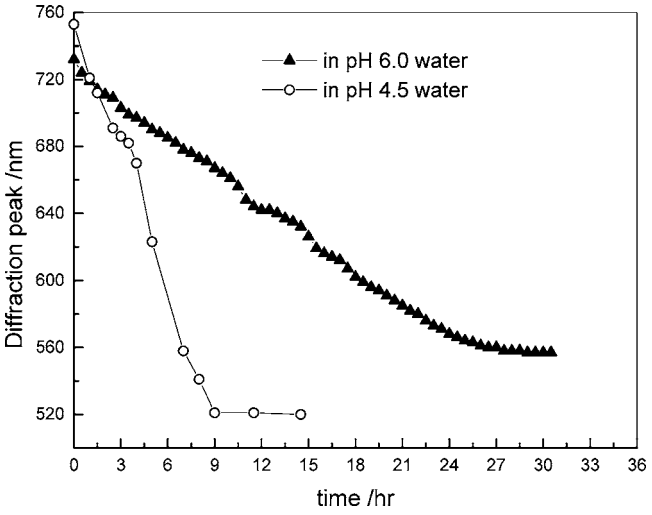

Figure 11. Time dependence of diffraction wavelength of HEMA PCCA gel containing 5.6 mol % sodium carboxylates. The PCCA gel was dispersed in either a pH 6.0 or pH 4.5 water reservoir where $V_{bath}/V_{gel} = 8 \times 10^4$.

by titrating the PCCA in pure water with HCl. We then increased the pH by adding aliquots of NaOH and again measured the diffraction after a 1 h delay.

As shown in Figure 10, we found a hysteresis in the pH response. The apparent pK_a is close to 8.8 on acid titration but close to 5.0 upon base titration. It should be noted that a similar but much smaller hysteresis was also previously observed in Braun et al.'s pH study of inverse opal hydrogels.[19]

This hysteresis results from the Donnan potential present in low ionic strength solutions; no hysteresis occurs in high ionic strength media. As noted by eq 6, the relative $[H^+]$ ion concentration within the PCCA compared to that in solution, $[H^+]/[H^+]^* = c^*_-/c_-$ depends upon the relative mobile anion concentrations in solution relative to that in the PCCA. Starting at high pH all carboxyl groups are in their anionic carboxylate form which repels mobile anions and localizes cations such as protons within the PCCA. This dramatically increases the $[H^+]$ ion concentration, effectively raising the carboxylate apparent pK_a to 9, compared to that expected of ~4. In the case of titrating from acidic to basic pH values the carboxyl groups are initially neutral, and no Donnan potential occurs to shift the apparent pK_a. When the volume of the bath reservoir becomes very large ($V_{bath}/V_{gel} = 8 \times 10^{10}$), the equilibrium pH difference between the inside and outside of the PCCA decreases, leading to a much smaller apparent hysteresis.

As shown in Figure 10 the modeled hysteresis is much smaller than we experimentally observed. This difference probably is due to the long times it takes to achieve ionic equilibrium. As pointed out by Tanaka,[18] the efficient diffusion rate of ions (H^+) inside the polyelectrolyte gel is greatly decreased within an anionic hydrogel. The estimated equilibration time is:

$$\tau = \left(\frac{V}{V_0}\right)^{2/3} \frac{l_0^2}{D_{H^+}} \left(1 + \frac{[A]}{K_a}\right) \approx 6.6 \text{ h}$$

where $l_0 = 125$ μm is the PCCA thickness, $D_{H+} = 8 \times 10^{-5}$ cm^2/s is the H^+ diffusion rate in water, $V/V_0 \approx 1.4$ is the ratio of final and initial PCCA volume, [A] = 0.156 M is the concentration of carboxyl groups in the PCCA, and $K_a = 1.6 \times 10^{-5}$ is the dissociation constant of the carboxyl groups. The estimated 6.6 h equilibrium time agrees with the results of Figure 11, where we placed a PCCA hydrogel poised at pH = 10 into either a pH 6.0 or pH 4.5 water solution ($V_{bath}/V_{gel} = 8 \times 10^4$) and observed the diffraction wavelength as a function of time.

The initial diffraction occurred at 738 nm and shifted over the first hour (corresponding to the time we waited to measure data in Figure 10) to 721 nm. The diffraction wavelength continued to blue-shift and after 12 h stabilized at 579 nm, which is close to the modeled results (585 nm) as shown in Figure 10. In pH 4.5 water, the PCCA reached equilibrium ($\lambda = 520$ nm) much faster. We also found that PCCA with all carboxylic groups responded to pH change much faster, stabilizing in minutes

Conclusions

We have synthesized HEMA PCCA hydrogels where the embedded CCA array consists of monodisperse highly sulfonated silica spheres. We dissolved out the silica spheres with HF to form a PCCA of water holes. This PCCA acts as a very sensitive sensor for the presence of ethanol due to a more favorable free energy of mixing for the HEMA with the ethanol. We demonstrated that we can use Flory hydrogel theory to model the hydrogel volume changes due to changes in the Flory−Huggins χ parameter as ethanol is added.

We also carboxylated these HEMA PCCA and discovered a large hysteresis behavior for acid vs base titration, which results from ultraslow kinetics (~1 day) for achieving ionic equilibrium because of ultraslow proton diffusion in these anionic hydrogels. This has important consequences in the transport of ions in hydrogels.

Acknowledgment. We gratefully acknowledge financial support from NIH Grant 2 R01 EB004132.

JA077979+